Progress in MJ plasma focus research at IPPLM

**Marek Scholz,
Lesław Karpinski,
Viacheslav I. Krauz,
Pavel Kubeš,
Marian Paduch,
Marek J. Sadowski**

Abstract. The results of studies of the plasma dynamics and neutron emission on a PF-1000 facility in the stage of pinch formation are presented. The measurements were performed using various modifications of the calibrated magnetic probes, 16 frame interferometry, silver activation counters and photomultiplier tube (PMT) neutron probes. The current measurements at a distance of 40 mm from the axis of the electrodes was measured. This dependence agrees well with the known scaling, $Y_n \sim I^4$. The evolution of plasma density during pinch formation and a neutron emission were study.

Key words: plasma focus • PF-1000 facility • magnetic probes • interferometry • neutron yield scaling

M. Scholz✉, L. Karpinski, M. Paduch
Division of Magnetised Plasma,
Institute of Plasma Physics and Laser Microfusion,
Association EURATOM-IPPLM,
23 Hery Str., 01-497 Warsaw, Poland,
Tel.: +48 22 638 1005 ext. 26, Fax: +48 22 666 8372,
E-mail: marek.scholz@ifpilm.pl

V. I. Krauz
National Research Centre "Kurchatov Institute",
1 Kurchatova Str., 123182 Moscow, Russia

P. Kubeš
Czech Technical University (CVUT),
2 Technicka Str., 166 27 Prague 6, Czech Republic

M. J. Sadowski
Division of Magnetised Plasma,
Institute of Plasma Physics and Laser Microfusion,
Association EURATOM-IPPLM,
23 Hery Str., 01-497 Warsaw, Poland
and National Centre for Nuclear Research (NCBJ),
7 Andrzeja Sołtana Str., 05-400 Otwock/Świerk, Poland

Introduction

The well-known feature of a Plasma-Focus (PF) system is the strong dependence between the current flowing in a pinch and the intensity of ionizing radiation emitted from the pinch. Especially, the experimental neutron scaling law based on measurements performed on devices with condenser banks of energy from few to hundreds kJ was expressed by $Y_n \sim I^{3.3-5}$ [5]. Later investigations, however, carried out on MJ devices showed [2, 3] that there is a certain condenser bank energy limit above which the scaling law is not valid and the neutron yield stabilizes at a level of 10^{11}–10^{12} neutron/shot.

Since, for the last few years, research on MJ plasma focus has been dealing with the following problems:
– Which physical mechanisms determine high efficiency of neutron production for such a configuration.
– What is the reason of the saturation effect of neutron production vs. current.

This effect of saturation can appear when a part of all PF current flows outside a PF pinch. Measurements of current distribution carried out in a Frascati megajoule PF experiment showed that a part of all current flowed in the rest plasma near insulator of the megajoule PF and did not participate in pinch compression [2].

The mentioned points touches the understanding of physics which dominates the plasma formation. This question is closely related to neutron production mecha-

nisms, plasma dynamics and physics of the conversion of magnetic field energy into pinch plasma energy.

The scope of this paper is to demonstrate the experimental results of high-current PF discharges devoted to character of the neutron emission. Experimental studies were carried out with different diagnostic techniques, i.e. a Mach-Zehnder interferometer (16 frames), fast scintillation probes for X-ray and neutron detection, specially prepared absolute calibrated magnetic probes (ACMP). The recent studies have been carried out mostly with a pure deuterium filling, and particular attention was paid to the correlations between the fast-neutron emission and the evolution of plasma parameters. The total fusion--neutron yield, as measured with four silver-activation counters, was found to be up to 7×10^{11} per shot, depending on the experimental conditions. Correlations of the neutron pulses with interferometric frame-pictures of the PF pinch column were studied. From time-of-flight (TOF) measurements of the fusion neutrons it was possible to estimate an energy spectrum of deuterons involved in the D-D reactions. Recently, the fast fusion-produced protons have also been recorded and analyzed by means of pinhole cameras and shielded track detectors.
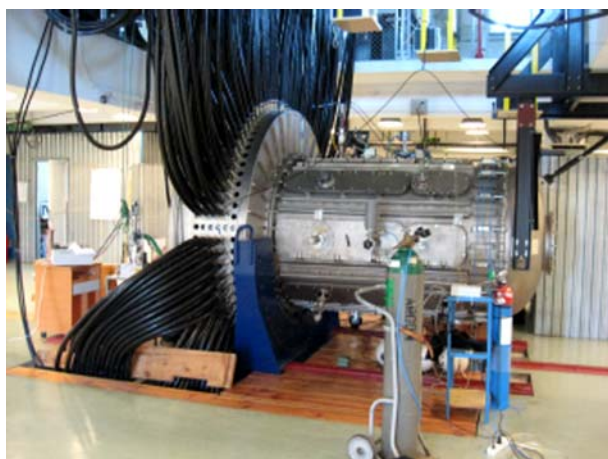
The PF-1000 facility

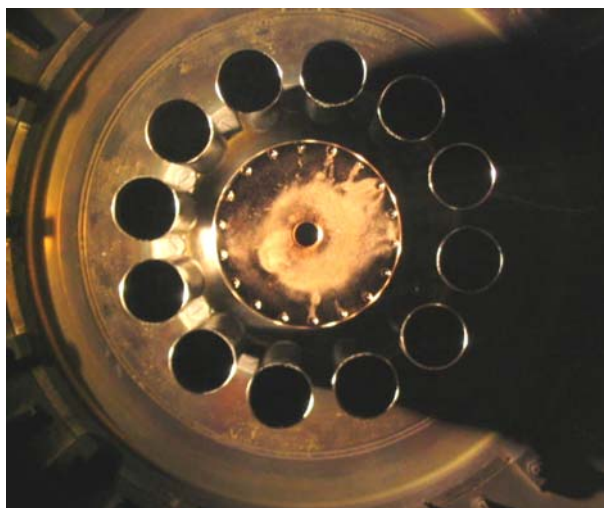The large scale PF-1000 facility (see Fig. 1) consists of the following main units:
– the condenser bank and pulsed electrical power circuit with a collector and low-inductance cables,
– the mechanical vacuum and gas system consisting of a vacuum chamber, coaxial electrodes and a gas handling system.

The electrical energy is transferred to a collector and electrodes by means of low-inductance cables. The vacuum chamber, which surrounds the electrodes, has a large volume (1400 mm in diameter and 2500 mm in length). Two coaxial electrodes are shown in Fig. 2.

The outer electrode (cathode) consists of 12 stainless steel rods of 80 mm in diameter. The outer electrode (OE) and copper centre electrode (CE) radii are 200 and 115.5 mm, respectively with a CE length of 46 cm. The cylindrical alumina insulator sits on the CE and the main part of the insulator extends 8.5 cm along the CE into the vacuum chamber. The insulator

Fig. 2. View of the PF-1000 electrodes.

prescribes the shape of the initial current sheet between the CE and the back plate of the OE.

The condenser bank of capacitance 1332 µF was charged to voltage ranging between 20–40 kV, which corresponded to discharge energies ranging from 266 to 1064 kJ.

During the described experiment, the total energy stored in the bank was 485 kJ, while the working gas was deuterium. Several shots with a 2 MA peak current and a 5–6 µs quarter period were made. The initial deuterium pressure was changed between 2 and 4 hPa.

Experimental arrangements

To study the evolution of the pinch plasma, a sixteen--frame Mach-Zehnder interferometer with an exposure time of about 1 ns was employed (see Fig. 3). In the case of the interferometer the ND:YLF laser is used as a light source. The laser can emit light with base wavelength (1.06 µm) or the 2nd, 3rd and 4th harmonic of the base frequency. The 2nd harmonic was used to obtain inteferograms. An optical delayed line allows for spatial selection between frames delays in the range from 0 to 220 ns, the delay between subsequent frames being in the range 10–20 ns. The detailed description of the interferometer setup is presented in [7].

To determine a current flowing near the pinch under the PF discharge conditions on the PF-1000 facility,

Fig. 1. View of the PF-1000 vacuum chamber, collector and HV cables.
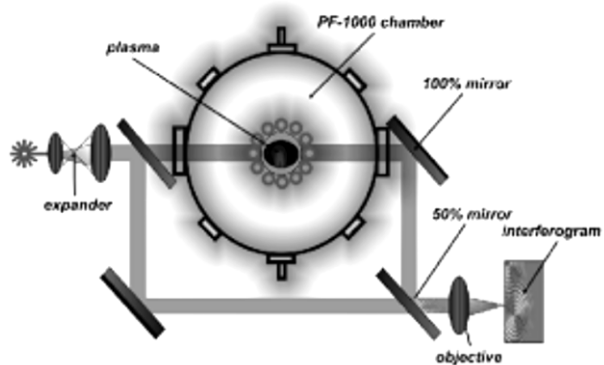
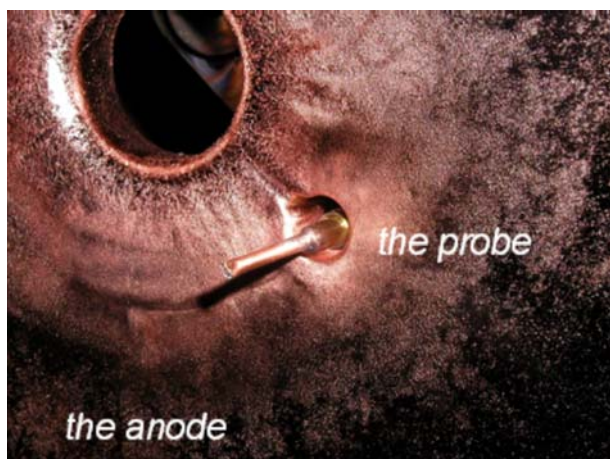**Fig. 3.** Mach-Zehnder interferometer setup for PF-1000U [7].

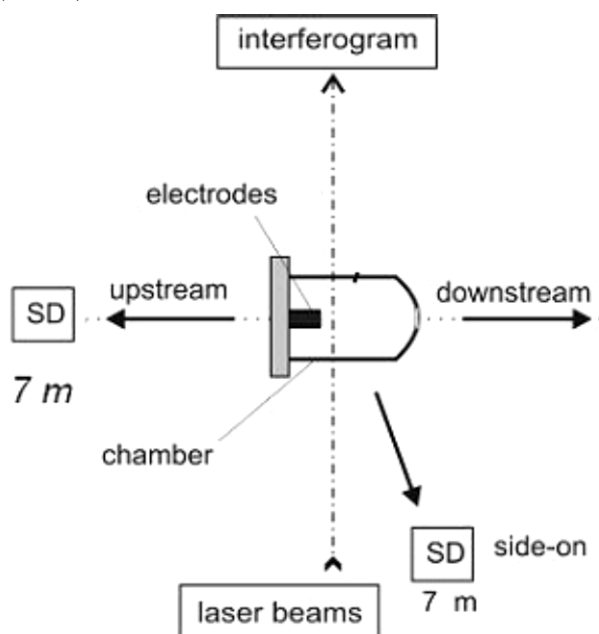**Fig. 4.** Setup of the absolute calibrated magnetic probe (ACMP).

Fig. 5. The arrangement of neutron probes.

modified and absolutely calibrated magnetic probes (ACMP) were designed and manufactured [1]. The probes designed for measurements in the stage of current sheath compression in the PF-1000 facility consist of two ~ 300-μm-diameter coils wound in clockwise and counterclockwise directions. They were located 40 mm from the electrode axis (Fig. 4).

In addition, the following standard electrical diagnostics applied on PF-1000 were used:

– *dI/dt* of the total discharge current was measured using three single-loop magnetic detectors located inside the collector of PF-1000. The detectors were arranged with a step of 120° along the collector perimeter, which made it possible to estimate the current homogeneity at the collector.
– The interelectrode voltage was measured by a capacitive divider mounted inside the collector with a sensitivity of 4 kV/V.
– The total discharge current was recorded using a calibrated Rogowski coil with a sensitivity of 470 kA/V.

During the experiment, the two following characteristics of neutron emission were measured:

– A total neutron yield was recorded using four silver activation counters. The counters were calibrated in their standard positions in the previous PF-1000 experiments.
– A time-resolved emission of neutron and hard X-ray radiation was registered by two fast scintillation probes (FNSP-1) based on the classical PMT with a BC-408 plastic scintillator. These probes were installed at a distance of 7 m end-on (upstream) and side-on from the anode plate of the PF-1000 (Fig. 5).

The integral neutron yield in these experiments was the main parameter characterizing the discharge quality. In combination with magnetic probe measurements, it allows one to analyze the neutron scaling in terms of the discharge current. Furthermore, a time--resolved measurements of neutron were correlated with interferometric frames, so the emission of neutrons is connected with evolution of the pinch plasma.

Measurements results of an azimutal magnetic field and a neutron yield

Figure 6 shows the signals recorded by absolute calibrated magnetic probes fixed at a distance of 4 cm from the PF axis (see Fig. 4). Presented signals were obtained in dischargers with a low (10^8 neutrons/shot) and high (10^{11} neutrons/shot) neutron yield. Thus, the probe
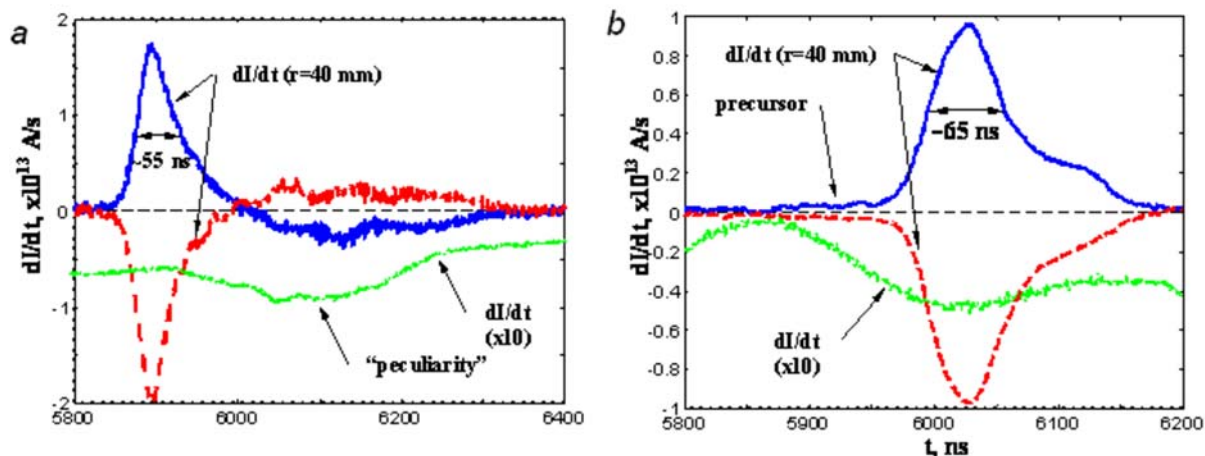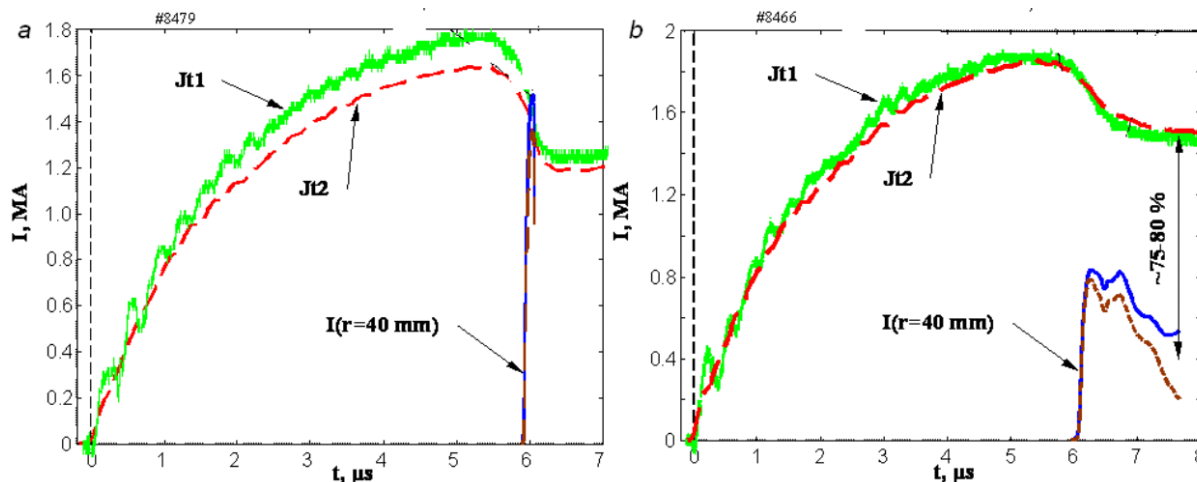

Fig. 6. Results of measurement of the azimuthal magnetic field during two discharges: a – shot 8479 (D$_2$, p_0 = 2.66 mbar, U_0 = 23 kV, Y_n = 1.0 × 10^{11}), and b – shot 8466 (D$_2$, p_0 = 2.66 mbar, U_0 = 24 kV, Y_n = 1.5 × 10^8).

Fig. 7. Currents measured by means of the Rogowski coil (Jt1), a single-loop (Jt2) and a probe located at $r = 40$ mm, a – shot 8479 (D_2, $p_0 = 2.66$ mbar, $U_0 = 23$ kV, $Y_n = 1.0 \times 10^{11}$), b – shot 8466 (D_2, $p_0 = 2.66$ mbar, $U_0 = 24$ kV, $Y_n = 1.5 \times 10^8$).

located at a distance of 4 cm from the PF axis, near the pinch, did not affect on pinching process. It follows from Fig. 6 that the signals from two different probe coils remain practically symmetric, which confirms their magnetic nature. The full width at half-maximum (FWHM) of each peak signal being ~ 50–65 ns.

The current strength values were calculated on the basis of the measured induction of the azimuthal magnetic field. The results of the calculation are presented in Fig. 7, where the current measured by the Rogowski coil and a single-loop magnetic detector located inside the collector also are shown.

One can see from Fig. 7 that the probe located at a radius of 4 cm recorded sometimes only about one--half of the total current measured by the Rogowski coil (Fig. 7b). It means a shunting of the main current channel. Due to the shunting of the main current channel, the fraction of the current compressed to the axis decreases substantially, which resulted in a reduction of the neutron yield. In other case, the probe recorded the total current measured by the Rogowski coil (Fig. 7a) and an important consequence of this result is that the discharge current is efficiently compressed toward the axis (at least to a radius of 4 cm), which results in the high value of neutron yield in this discharge. These above results demonstrate the problem of the efficiency of discharge current transportation toward the axis. Figure 8 shows
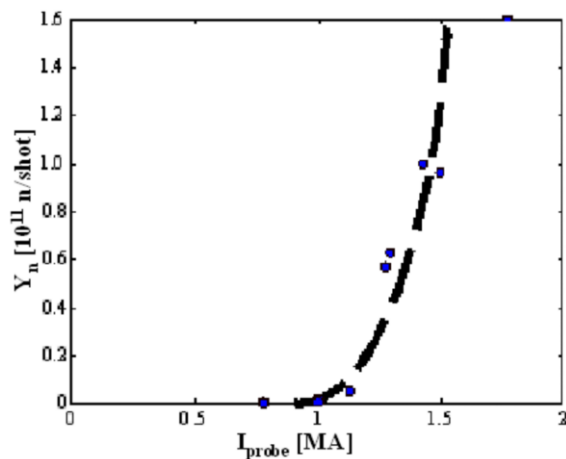
the measured neutron yield as a function of the current measured by a probe installed at a radial distance of 40 mm from the axis.

One can see that the curve in Fig. 8 shows the scaling I^4. It means, that the high neutron yields correspond to the high efficiency of current compression onto the axis, as is observed, e.g., in Fig. 7a. In the opposite case one can note that, in some discharges, the neutron yield is very low in spite of the high value of the total discharge current measured by the Rogowski coil. This fact is related to the secondary shunting breakdowns, due to which only a lower fraction of the total current contributes to the pinch formation (Fig. 7b).
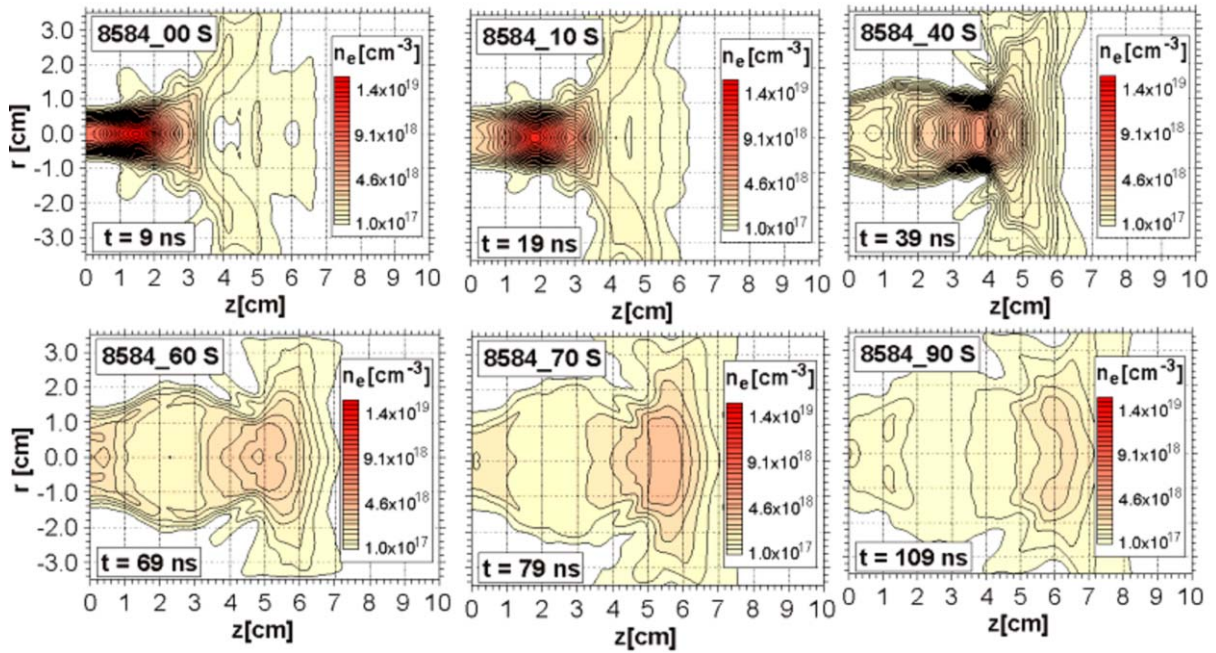
Results of measurement of a pinch density and neutron emission

Figure 9 shows the evolution of density during shot with a high neutron yield. The electron density distributions in the pinch plasma was reconstructed on the basis of interferograms using the method described in a previous paper [4].

It is seen that the pinch diameter is about 1.6 cm at 9 ns after the minimum of the current derivative, its length is 3–5 cm, and the maximum electron density of the pinch column amounts to ~ 2×10^{19} cm^{-3}. The stage of the pinch stagnation lasts 10 ns and the pinch plasma moves axially from the anode during the stage. After that, from the moment on 39 ns the radius of the pinch column grows continuously with a diminishing of the plasma electron density. One did not observe a grow of the sausage instability in the shot #8584.

To study anisotropy of a neuron emission during the shot 8584, the neutron output was recorded by PMT probes located at a distance of 7 m side-on and in the upstream directions (see Fig. 5). Figure 10 shows the result of the recording.

The character of hard X-ray (HXR) and neutron pulses in the shot 8584 is not typical as described in [6], because four HXR and neutron pulses were detected and the first neutron pulse is dominant and isotropic. The neutron yield in the shot was $Y_n = 4.2 \times 10^{11}$. However, for other shots the evolution of the pinch plasma is more conventional (Fig. 11).


Fig. 8. Neutron yield Y_n as a function of (a) the maximum current recorded by the magnetic probe at a radius of 40 mm.

Fig. 9. Shot 8584 (D₂, p_0 = 2.4 mbar, U_0 = 27 kV, Y_n = 4.2 × 10¹¹). Equidensity contours reconstructed from interferograms taken at different moments after the minimum of dI/dt.
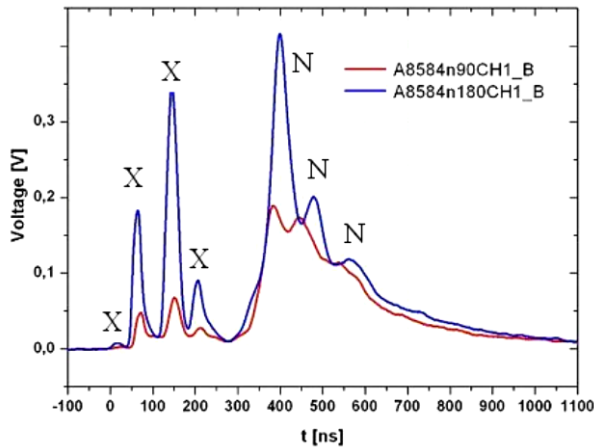
**Fig. 10.** Shot 8584 (D₂, p_0 = 2.4 mbar, U_0 = 27 kV, Y_n = 4.2 × 10¹¹). Four hard X-ray (X) and neutron (N) pulses recorded by PMT probes side-on (A8584n90CH1_B) and upstream (A8584n90CH1_B).

Figure 11 shows the late stage of a pinch history when sausage instability appears. A character of HXR and neutron pulses in the shot 8406 is demonstrated in Fig. 12. There exist generally at least two distinct neutron pulses, where the second correlate to stage of sausage instability.

The neutron yield in the shot was Y_n = 9.0 × 10¹⁰. To study anisotropy of a neuron emission during the shot 8406, the neutron output was recorded by PMT probes located at the same position like a shot 8584 (see Fig. 5). Figure 12 shows the result of the recording. One can see shots without sausage instability and with an isotropic energy spectrum of the neutron emission. One can also observe other shots with a sausage instability after the pinch stagnation and an anisotropic energy spectrum of neutrons. It is shown evidence of beam target processes.
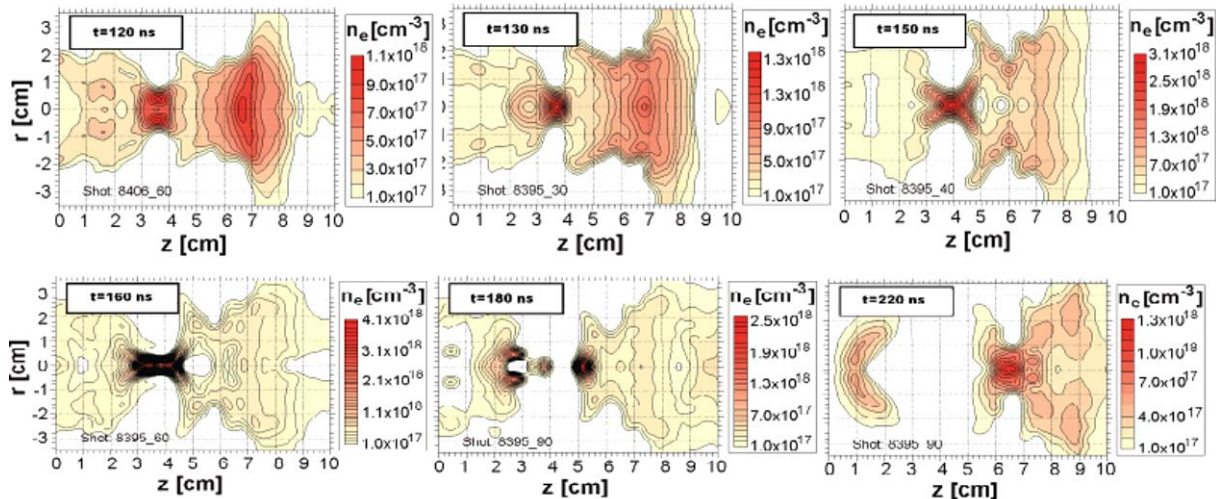
Fig. 11. Shot 8406 (D₂, p_0 = 2.4 mbar, U_0 = 24 kV, Y_n = 9.0 × 10¹⁰). Equidensity contours reconstructed from interferograms taken at different moments after the minimum of dI/dt.
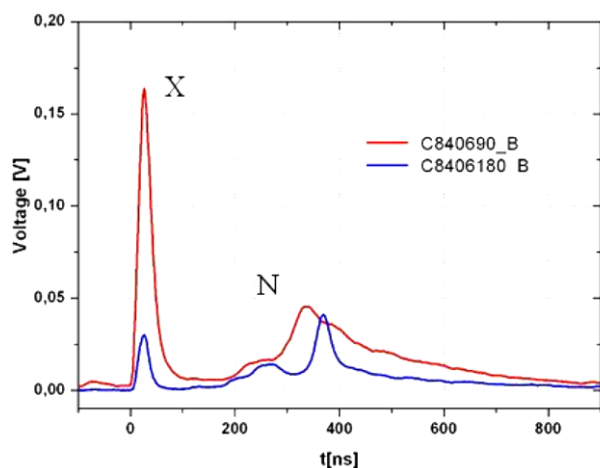
Fig. 12. Shot 8406 (D$_2$, p_0 = 2.4 mbar, U_0 = 24 kV, Y_n = 9.0 × 10^{10}). Hard X-ray (X) and neutron (N) pulses recorded by PMT probes side-on (C8406n90_B) and upstream (C8406n180_B).

Conclusions

It is shown that the current flowing in the converging sheath at a distance of 40 mm from the axis of the facility electrodes is equal to the total current in the optimal operating modes, which indicates the high efficiency of current transportation toward the axis. It is shown that the neutron yield depends on the current compressed onto the axis. This dependence agrees well with the known scaling $Y_n \sim I^4$.

Additionally, two modes of the PF-1000 operation were found. One can see shots without sausage instability and with an isotropic energy spectrum of the neutron emission. One can also observe other shots with a sausage instability after the pinch stagnation and an anisotropic energy of neutron emission. In this shots specific beam target processes are of importance, but for the previous one the situation is not clear. The relative ratio between two kind of shots is hard to determine because the statistics of shots with interferometry is poor. So, the problem of neutron production mecha-

nism in a pinch plasma seems still open, but we can propose hypothesis that the spatial distribution of the plasma density and current in the final stage of plasma compression influence the processes responsible for magnetic energy dissipation, plasma stability and emission of neutrons.

Unfortunately, it is hard to say which type of discharge corresponds to the data presented in Fig. 8, because the interferometry has not been used during the experimental session, when the data have been collected.

References

1. Frolov I, Grabovski E, Mitrofanov K, Oleinik GM, Smirnov VP, Zukakishvili GG (2001) Magnetic field measurements inside and outside of imploding arrays on Angara-5-1. In: Scott PE (ed) Proc European Conf Advanced Diagnostics for Magnetic and Inertial Fusion. September 3–7, 2001, Villa Monastero, Varenna, Italy. Academic/Plenum Publishers, 1:419–422
2. Gourlan C, Kroegler H, Maisonnier C, Rager JP, Robouch BV, Gentilini A (1979) Recent progress in 1-MJ Plasma Focus dynamics and scaling for neutron production. In: Proc of the Int Conf on Plasma Physics and Controlled Nuclear Fusion Research. Vol. II. IAEA, Vienna, 1:123–134
3. Herold H, Jerzykiewicz A, Sadowski M, Schmidt H (1989) Comparative analysis of large plasma focus experiments performed at IPF Stuttgart and at IPJ Świerk. Nucl Fusion 29:1255–1266
4. Kasperczuk A, Pisarczyk T (2001) Application of automated interferometric system for investigation of the behaviour of laser-produced plasma in strong external magnetic fields. Opt Appl 31:571–597
5. Rager JP (1981) The Plasma Focus. Com Naz Energ Nucl Centr Frascati 81.19/cc
6. Schmidt H, Kubes P, Sadowski M, Scholz M (2006) Neutron emission characteristics of pinched dense magnetized plasmas. IEEE Trans Plasma Sci 34:2363–2367
7. Zielinska E, Paduch M, Scholz M (2011) Sixteen-frame interferometer for a study of a pinch dynamics in PF-1000 device. Contrib Plasma Phys 51:279–283